PROPELLERS IN COMPRESSIBLE FLOW

Valana L. Wells
Graduate Student
Stanford University
Stanford, California, USA

Abstract

This paper describes a method for solving the equation for inviscid, irrotational, compressible, potential flow about a propeller. The equation is written in a non-inertial system of coordinates rotating with the propeller in which the problem becomes a steady one. The solution is constructed by superimposing a solution to the compressible equation on an "incompressible" or "wake" solution. A "modal" or "shape" function method provides a procedure for solving the integral equation resulting from application of the final boundary condition to the superposed solution. Results are presented for an increasing number of control points and modal functions. A comparison of compressible and incompressible circulation distributions is also included.

Symbols

a speed of sound
A series coefficient
B number of blades; series coefficient
c blade chord
g shape function coefficient
M axial Mach number $= \frac{U}{a}$
p source distribution
r dimensional radial coordinate
R potential function of ρ; tip radius
t time
u perturbation velocity
U axial free stream velocity
v_i perpendicular induced velocity at blade
V total velocity (inertial system)
w wake velocity
W total velocity (rotating system)
α angle of attack
β $\sqrt{1-M^2}$
γ Hankel transform variable
Γ circulation
Γ^* dimensionless circulation $= \Gamma \frac{\omega}{U^2}$
ϵ helix angle $= tan^{-1}\frac{U}{\omega r}$
ς helical coordinate $= \theta - z$
θ angular coordinate
μ density
ρ dimensionless radial variable
σ helical coordinate $= \theta + z$
φ perturbation velocity potential
Φ total velocity potential
ω propeller angular velocity

Subscripts

i incompressible
c compressible
n nth term in a series
s sonic

Superscripts

$\tilde{}$ quantity in inertial coordinates
$\bar{}$ Hankel transformed quantity; dimensionless quantity
$\vec{}$ vector
$'$ perturbation quantity; inner Hankel integral form
$+$ ahead of propeller
$-$ behind propeller
$*$ dimensionless quantity

1. Introduction

A large number of propeller analysis methods exist, and designers currently use nearly all of them to some extent. The methods have enjoyed varying degrees of acceptance, largely due to their great variation in complexity and the corresponding variation in accuracy.

The Blade Element–Momentum method is, perhaps, the most widely used since it is easily implemented. It roughly corresponds to the strip theory for wings and, like the strip theory, does not account for the effects of aerodynamic induction. Vortex methods encompass those which compute induced velocities due to a trailing vortex system. This idea, attributed to Betz and recounted by Prandtl[1], has been implemented by direct solution of the governing potential equation – Goldstein[2], Reissner[3], and Theodorsen[4] – and by computation of induced velocities by the law of Biot and Savart – Glauert[5] and, more recently, Shiao, Chang et. al., and Glatt et. al. (refs. 6–9). The above methods basically deal with incompressible flow, though empirical or semi-empirical Mach numbe corrections may be incorporated into them.

Three authors in particular have had some success using the method of matched asymptotic expansions in the analysis of rotors. Pierce and Vaidyanathan [10] studied incompressible, unsteady, helicopter–type rotor blades using

this approach. Johansson[11] used matched asymptotic expansions to study helicopter–type rotors and propellers in compressible, steady flow.

Propellers have been analyzed using computational fluid dynamical methods with, so far, limited success (ref. 12). C F D, however, promises better results in the future for accurate propeller flow field prediction.

Potential singularity methods, including various forms of lifting surface and paneling techniques, comprise the most popular of the advanced propeller analysis methods. Ffowcs Williams and Hawkings[13] developed the foundation of this approach for surfaces in arbitrary motion, though their work particularly related to acoustic theory. Most aerodynamic applications utilize only the mono– and dipole solutions (sources and doublets), neglecting the nonlinear quadrupole solution. Further relevant acoustic– related work was done by Farrasat[14] and Schmitz and Yu[15]

Several authors have pursued the potential singularity approach from the aerodynamic standpoint. Dat[16] and Runyan[17] developed a general lifting surface theory for wings and propellers in compressible, unsteady flow. The incompressible propeller cases were specialized by Kerwin [18] (steady), Summa[19] (unsteady), and Jacobs and Tsakonas[20] (unsteady). Long[21] specifically used Ffowcs Williams–
Hawkings acoustic singularities to determine aerodynamic loads on propellers.

The Integral–Equation approach to the problem of computing the aerodynamics of propellers has been extensively studied. The kernel functions for all cases above have been determined and most have been implemented for purposes of application. Unfortunately, the lifting surface/kernel method for rotors has proven tedious due to the large number of control points required for accurate calculations. The present work focuses on an alternative solution method for finding aerodynamic loads on a propeller in order to simplify the computational procedures and requirements.

Most of the theories mentioned above were developed for an observer in an inertial reference frame. Transferring the problem to a coordinate system rotating with the propeller leads to the ability to treat the boundary conditions as steady ones (uniform inflow) or, at least in the same terms as those for a vibrating wing (non–uniform inflow or vibrating blade). In this non–inertial reference frame, the Integral–Equation approach is still valid, but with the potential doublet transferred to the rotating system. However, in attempting to avoid the computational complexities of kernel function solution, this work deals directly with solving the compressible potential equation in rotating coordinates.

Davidson[22] and Busemann[23] studied this problem for the case of a propeller in a wind tunnel. The work in this paper is based on their approach, but with boundary conditions suitable to a propeller operating in free air. The method is applicable to unsteady flow about propellers, but only the steady case is extensively studied here.

2. Development of the Compressible Flow Equation for Propellers in Potential Flow

Except in the vicinity of the propeller and its wake, the flow field due to a advancing propeller in a space–fixed, or inertial, coordinate system may be considered irrotational and isentropic. This approach treats the viscous drag on the blade as inconsequential to the general theory. Given a total potential, Φ, of the total velocity $\vec{V}$, the governing equation of the flow is

$$\nabla^2\Phi = \frac{1}{a^2}(\vec{V}\cdot\frac{D\vec{V}}{Dt} + \frac{\partial}{\partial t}\frac{V^2}{2} + \frac{\partial^2\Phi}{\partial t^2}).$$

The velocity in the inertial system may be written as a superposition of the oncoming velocity, $U\hat{k}$, and the perturbation, $\vec{u}'$. As long as all components of $\vec{u}'$ are small relative to U, the linearized version of the above equation applies. The assumption of small $\vec{u}'$ implies that the induced velocity due to rotation of the propeller blade must be small compared with U. It can be argued for thin blade airfoils that $|\vec{u}'|$ will always be much less than $\sqrt{\omega^2r^2+U^2}$ where ω is the propeller angular velocity. However, to ensure $|\vec{u}'| << U$, the oncoming velocity must be on the same order as ωr. Thus, the linearized analysis holds only for lightly–loaded, or high advance ratio, propellers.

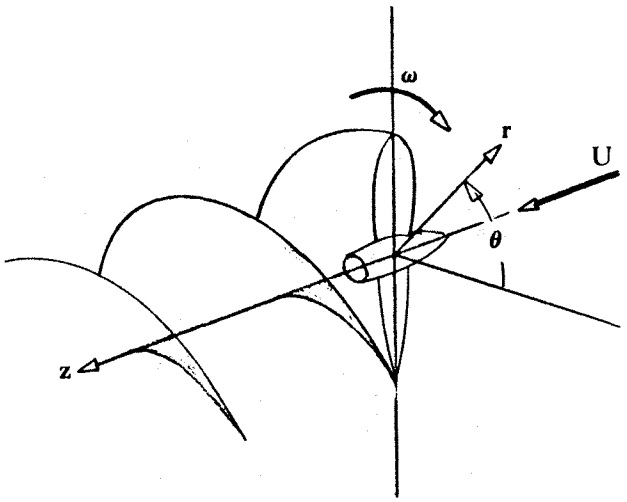

Figure 2.1 -- Coordinate System

Assuming, then, high advance ratio, the above equation reduces to

$$\nabla^2\tilde{\varphi} - M^2\frac{\partial^2\tilde{\varphi}}{\partial\tilde{z}^2} = \frac{1}{a^2}(2U\frac{\partial^2\tilde{\varphi}}{\partial\tilde{z}d\tilde{t}} + \frac{\partial^2\tilde{\varphi}}{\partial\tilde{t}^2}), \qquad (2.1)$$

where $\tilde{\varphi}$ now represents the perturbation velocity potential $\tilde{z}$ and $\tilde{t}$ refer to the variables in a translating coordinate system, and a represents the ambient speed of sound.

Though equation (2.1) above is usually derived in a Cartesian system of coordinates, one can show that the same equation holds, to first order, in th cylindrical system, $(\tilde{r},\tilde{\theta},\tilde{z})$, since the variations occur only in higher order terms. The Laplacian, however, must be considered in cylindrical coordinates. Note that a boundary condition to (2.1) must specify tangency of flow at the rotating propeller blade.

Conversion to Rotating Coordinates

Consider a transformation to a blade-fixed coordinate system which rotates with the propeller at angular velocity, ω. This non-inertial system, (r, θ, z, t), is defined by:

$$r = \tilde{r}, \quad \theta = \tilde{\theta} + \omega\tilde{t}$$
$$z = \tilde{z}, \quad t = \tilde{t}.$$

Performing these coordinate transformations gives the unsteady, linearized potential equation in the rotating system:

$$\nabla\varphi = M^2\frac{\partial^2\varphi}{\partial z^2} + 2MM_\theta\frac{1}{r}\frac{\partial^2\varphi}{\partial z\partial\theta} + M_\theta^2\frac{1}{r^2}\frac{\partial^2\varphi}{\partial\theta^2} + \frac{1}{a}\left\{2U\frac{\partial^2\varphi}{\partial z\partial t} + 2\omega\frac{\partial^2\varphi}{\partial\theta\partial t} + \frac{\partial^2\varphi}{\partial t^2}\right\}, \tag{2.2}$$

where $M_\theta \equiv \frac{\omega r}{a}$ is the radially varying apparent Mach number in the angular direction.

Boundary Conditions

In general, the solution to a linearized lifting body problem is subject to the following conditions:

1.) Tangency of the flow at the body surface;

2.) Vanishing (or at least finiteness) of disturbances an infinite distance away from the body and its wake; and

3.) Zero normal velocity through the wake.

The first of these conditions has the mathematical representation (see, for example, Dowell,[24]):

$$\frac{\partial F}{\partial\tilde{t}} + \vec{V}\cdot\nabla F = 0 \; on \; F = 0,$$

where $F = 0$ represents the surface of the lifting body, and $\vec{V} = \nabla\Phi$ is the total velocity vector in an inertial coordinate system. By the rule for vector time derivatives, in a non-inertial frame, the total velocity, as seen in the coordinate system rotating with angular speed, ω, is:

$$\vec{W} = \vec{V} - \vec{\omega}\times\vec{r} = \vec{V} - \omega r\hat{\theta}.$$

Substitution into the above boundary condition, along with the conversion of the time derivative, gives the boundary condition in the rotating reference frame:

$$0 = \frac{\partial F}{\partial t} - \omega\frac{\partial F}{\partial\theta} + \vec{W}\cdot\nabla F = \frac{\partial F}{\partial t} + \vec{W}\cdot\nabla F \quad on \quad F = 0,$$

which is the expected result. In other words, the body boundary condition may be treated in the same manner in the rotating coordinate system as it is in the inertial system, as long as the local freestream velocity, $\vec{W}$, is considered.

The wake boundary condition can be made mathematically tractable by assuming -

1.) Unsteady perturbations are small so that the unsteady wak has, to leading order, the same shape as the steady wake; and

2.) The slipstream velocity, w, is much smaller than the freestream velocity, U.

With these assumptions, the position of the wake can be approximated by:

$$\theta - \frac{\omega}{U}z = (n-1)\frac{2\pi}{B}, \quad r < R,$$

for $B \equiv$ the number of propeller blades, $n \equiv$ the blade index, and $R \equiv$ the blade radius. For $r = r_o$ and $n = 1$, for example, the equation describes a single helix with radius r_o and origin at $\theta = 0$. The wake surface is a helicoid made up of an infinite number of these helices with radii from $r = 0$ to $r = R$ originating at $z = 0$ and at each angular station corresponding to a propeller blade location.

The first order analysis assumes that all motion of the helicoidal wake occurs in the axial direction. Since there can be no flow through the wake, the wake condition is expressed as

$$w\,cos\,\epsilon = u_z\,cos\,\epsilon - u_\theta\,sin\,\epsilon$$

on

$$\theta - \frac{\omega}{U}z = (n-1)\frac{2\pi}{B}, \; r < R.$$

where $u_z \equiv$ induced velocity in the z-direction, $u_\theta \equiv$ induced velocity in the θ-direction, and $\epsilon \equiv$ helix angle $= tan^{-1}\,U/\omega r$. In terms of the velocity potential, then, the boundary condition is

$$\omega r w = \omega r\frac{\partial\varphi}{\partial z} - \frac{U}{r}\frac{\partial\varphi}{\partial\theta}.$$

Steady Flow Equation

The remainder of this paper will focus on the aerodynamics of the steady propeller; that is, a rigid propeller experiencing a uniform inflow. These conditions allow the time dependent terms in equation (2.2) to be excluded since, now, the flow field appears steady in the rotating, translating coordinate system.

The dimensional spatial variables, r and z, have convenient dimensionless forms - $\rho = \omega r/U$ and $\bar{z} = \frac{\omega z}{U}$. Dropping the bar over the dimensionless z variable, the steady, potential equation becomes:

$$\frac{\partial^2\varphi}{\partial\rho^2} + \frac{1}{\rho}\frac{\partial\varphi}{\partial\rho} + \beta^2\frac{\partial^2\varphi}{\partial z^2} + \frac{1}{\rho^2}(1-M^2\rho^2)\frac{\partial^2\varphi}{\partial\theta^2} - 2M^2\frac{\partial^2\varphi}{\partial\theta\partial z} = 0, \tag{2.3}$$

with $\beta^2 = 1 - M^2$. Equation (2.3) appears to depend on one parameter (M) only. However, the advance ratio parameter is hidden in the dimensionless variables, ρ and z.

In "helical" coordinates described by $\varsigma = \theta - z$ and $\sigma = \theta + z$, equation (2.3) looks like

$$\varphi_{\rho\rho} + \frac{1}{\rho}\varphi_\rho + (1+\frac{1}{\rho^2})\varphi_{\varsigma\varsigma} + (1+\frac{1}{\rho^2} - 4M^2)\varphi_{\sigma\sigma} - 2(1+\frac{1}{\rho^2} - 2M^2)\varphi_{\varsigma\sigma} = 0.$$

Goldstein[2] shows that, in the far wake, the flow field depends only on the variables ρ and ζ. (ζ runs counter to a helix at a given radius.) This results from purely geometrical considerations, and therefore holds for both compressible and incompressible flows. Thus in the far wake,

$$\varphi_{\rho\rho} + \frac{1}{\rho}\varphi_\rho + (1 + \frac{1}{\rho^2})\varphi_{\zeta\zeta} = 0,$$

which is exactly the equation solved by Goldstein. This result is of interest on two accounts:

1) The perturbed flow in the far wake has an incompressible character which implies that quantities which depend only on the far wake are invariant from incompressible to compressible flow.

2) The far wake solution for a propeller in incompressible flow also satisfies the compressible equation.

Davidson pointed out the latter and used that fact in his study of the propeller in compressible flow in a wind tunnel. This study also utilizes the far wake solution as will be shown in Section 3.

Formulating the problem in a rotating coordinate systems leads to some mathematical consequences of interest. Because the freestream velocity in this case depends on radial position, that freestream velocity reaches the speed of sound at some "sonic radius." This radius forms the boundary of a circular cylinder parallel to the z–axis, termed the "sonic cylinder." The expression for the sonic radius is easily obtained –

$$r_s^2 = \frac{a^2 - U^2}{\omega^2};$$

or, in dimensionless terms,

$$\rho_s^2 = \frac{1}{M^2} - 1.$$

For a purely subsonic propeller, the tip radius, ρ_a, is less than ρ_s always. However, a solution of the equation describing the flow field created by that propeller must include consideration of the outer region as well as the subsonic one.

In the simpler case of rectilinear, compressible, potential flow, the character of the flow depends on the sign of the quantity, $1 - M^2$. For $(1 - M^2) > 0$, the flow is subsonic and of elliptic character, whereas, for $(1 - M^2) < 0$, or supersonic flow, the character is hyperbolic. It is expected, then, that the flow character in rotating coordinates will depen on the sign of $(1 - M^2 - M_\theta^2)$, which is positive for $\rho < \rho_s$ (elliptic) and negative for $\rho > \rho_s$ (hyperbolic). A flow of mixed character results from formulating the problem in rotating coordinates.

A hyperbolic flow region implies the existence of characteristics – in the present case characteristic surfaces – within that region. von Mises[25] outlines a general theory of characteristics with particular application to compressible fluid flow. Utilization of his methods verifies that characteristics occur for $\rho^2 > \frac{1}{M^2} - 1$. This formally validates the expected result mentioned above.

Further discussions of characteristics for three and higher dimensional problems are found in references 26 through 29. Though this approach for the compressible propeller problem in rotating coordinates seems promising, it will not be pursued further at this time.

3. Solution of the Equation

The problem of compressible, potential flow about a propeller reduces to that of solving a partial differential equation subject to certain boundary conditions:

$$\beta^2\varphi_{zz} + \varphi_{\rho\rho} + \frac{1}{\rho}\varphi_\rho + \frac{1}{\rho^2}(1 + \rho^2 M^2)\varphi_{\theta\theta} - 2M^2\varphi_{\theta z} = 0; \quad (3.1)$$

subject to

1. φ finite at $\rho = 0$,
2. Sommerfield radiation as ρ becomes infinite,
3. No flow through the propeller blades, and
4. No flow through the propeller wake.

As discussed previously, the solution to the equation for the incompressible velocity potential, $\varphi_i(\rho, \theta - z)$, also solves the compressible equation. Though it cannot capture the compressible effects at the propeller blades, this solution accurately describes the far wake flow. Thus, a superposition of a compressible solution, which accounts for effects near the blades but dies out in the far wake, on the incompressible solution also constitutes a solution to the linear differential equation. As will be shown later, the superposed solution is desirable in this case as the analyti form of the compressible solution does not lend itself well to satisfying the wake boundary condition.

Though most forms of the incompressible velocity potential, φ_i, are derived at an infinite distance behind the propeller plane, any form given as $\varphi_i(\rho, \theta - z)$ must solve equ. (3.1). However, in order for the superposed solution $\varphi = \varphi_c + \varphi_i$ to form a solution to the entire problem, the sum, $\varphi_i + \varphi_c$, must satisfy the boundary conditions. The first two conditions, finite φ at $\rho = 0$ and proper dying out of the disturbance as $\rho \to \infty$, do not cause any difficulty as they can be satisfied independently by φ_i and φ_c.

In order to account for the more problematic conditions (3) and 4) above), the flow field can be artificially divided into two regions – one forward of the propeller plane in which only the compressible velocity potential holds, and the other behind the propeller plane in which both φ_i and φ_c apply. The form of φ_i, which automatically provides for the existence of a trailing wake, necessitates the division of the flow field. This division, however, requires the introduction of two more "boundary" conditions which assure continuity at the propeller plane. Designating φ_c^+ as the forward potential and $\varphi^- = (\varphi_i + \varphi_c^-)$ as that behind the propeller, and situating the propeller at $z = 0$ as before, a continuous flow field is ensured by

$$\varphi_c^+ |_{z=0} = \varphi_i |_{z=0} + \varphi_c^- |_{z=0},$$

and

$$\frac{\partial \varphi_c^+}{\partial z} |_{z=0} = \frac{\partial \varphi_i}{\partial z} |_{z=0} + \frac{\partial \varphi_c^-}{\partial z} |_{z=0}. \quad (3.2.a, b)$$

Since both φ^+ and φ^- are valid at $z = 0$, both must satisfy the condition of no flow through the propeller blades.

The Incompressible Potential

Reissner[3] proposed a potential solution to the incompressible propeller problem which has a slightly simpler derivation than that given by Goldstein. Reissner's potential has the form:

$$\varphi = \varphi_o + \varphi_n$$

with

$$\varphi_o = \zeta R_o,$$

and

$\varphi_n = \sum_{n=1}^{\infty} R_n sin\ nB\zeta$. (B $\equiv$ number of blades.)

Reissner uses the potential φ_o to give the discontinuity distribution required along the helicoidal wake surfaces. He does this by requiring that

$$\nabla^2 \varphi_o = -q,$$

where q represents a source distribution on the helicoidal sheet describing the wake. In the case of a two-bladed propeller, for example, th source distribution at some $\rho < \rho_a$, as a function of ζ, looks qualitatively like a 2-cycle "sawtooth" function. (See Fig. 3.1.)

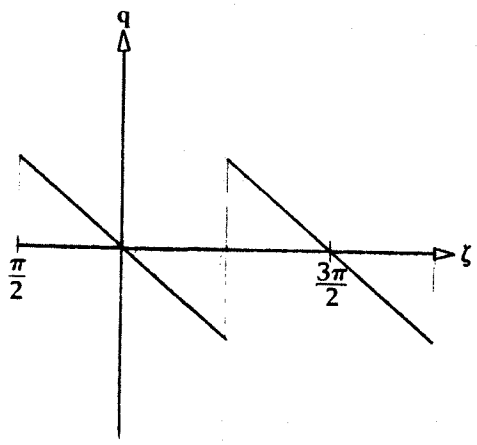

Figure 3.1 -- Assumed Source Distribution

Between sheets - for example - $-\frac{\pi}{2} < \zeta < \frac{\pi}{2}$ - q is linear in ζ so that

$$q = -k\zeta p(\rho).$$

In helical coordinates, the above Poisson equation becomes:

$$\varphi_{\rho\rho_o} + \frac{1}{\rho}\varphi_{\rho_o} + \left(1 + \frac{1}{\rho^2}\right)\varphi_{\zeta\zeta_o} = \frac{U^2}{\omega^2} q(\rho, \zeta).$$

So, letting $q = \frac{\omega^2}{U^2}\zeta p(\rho)$ and $\varphi_o = \zeta R_o(\rho)$, the solution for the velocity potential, φ_o becomes

$$\varphi_o = -\zeta \int_o^{\rho} \frac{d\xi}{\xi} \int_o^{\xi} \psi p(\psi)\psi.$$

Reissner computed φ_n so as to maintain $\nabla \cdot \bar{u} = 0$ in the flow field by requiring that $\nabla^2 \varphi_n = +q$. By assuming the series solution, $\varphi_n = -\sum_{n=1}^{\infty} R_n sin(nB\zeta)$, the expression for R_n becomes:

$$R_n = (-1)^n \frac{2}{nB}\Big\{a_n' I_{nB}(nB\rho) + a_n^2 K_{nB}(nB\rho) + I_{nB}(nB\rho)\int_o^{\rho} I_{nB}(nB\xi)\xi p(\xi)d\xi - K_{nB}(nB\rho)\int_o^{\rho} K_{nB}(nB\xi)\xi p(\xi)d\xi\Big\};$$

where the two integral terms represent particular solutions to the separated Bessel-Poisson equation in R_n.

This potential applies regardless of the boundary conditions which, of course determine values for the constants, a_n^1 and a_n^2. Free air boundary conditions result in

$$R_n = (-1)^n \frac{-2}{nB}\left\{K_{nB}(nB_\rho)\int_o^{\rho} I_{nB}(nB\xi)\xi p(\xi)d\xi + I_{nB}(nB_\rho)\int_{\rho}^{\rho_a} K_{nB}(nB\xi)\xi p(\xi)d\xi\right\},$$

It is generally convenient to describe the velocity potential in terms of the circulation distribution, $\Gamma(\rho)$, rather than the source strength. By definition, the circulation is equal to the discontinuity in potential across a sheet of vorticity. Thus,

$$\Gamma(\rho) = \Delta\varphi(\rho) = \frac{2\pi}{B} R_o = \frac{2\pi}{B}\int_o^{\rho}\frac{1}{\xi}\int_o^{\xi}\psi p(\psi)d\psi d\xi.$$

This gives a relationship between Γ and the source strength, p. Notice that the quantity φ_n does not contribute to the circulation strength since it does not have a discontinuity at the vortex sheet describing the wake.

Using the above expression, R_n can be written,

$$R_n = (-1)^n \frac{-B}{n\pi}\left\{K_{nB}(nB\rho)\int_o^{\rho} I_{nB}(nB\xi)d\left(\xi\frac{d\Gamma}{d\xi}\right) + I_{nB}(nB\rho)\int_{\rho}^{\rho_a} K_{nB}(nB\xi)d\left(\xi\frac{d\Gamma}{d\xi}\right)d\xi\right\}.$$

Integrating by parts,

$$R_n(\rho) = (-1)^n \frac{B}{n\pi}\left\{K_{nB}(nB\rho)\int_o^{\rho} I_{nB}\xi\frac{d\Gamma}{d\xi}d\xi + I_{nB}(nB\rho)\int_{\rho}^{\rho_a} K_{nB}(nB\xi)\xi\frac{d\Gamma}{d\xi}d\xi - I_{nB}(nB\rho)K_{nB}\xi\frac{d\Gamma}{d\xi}\Big|_{\xi=\rho_a}\right\}.$$

This latter form, though generally more easily dealt with numerically, may, in fact have a singularity at ξ or ρ equal to ρ_a. This occurs due to the form of the circulation distribution, $\Gamma(\rho)$, which often is assumed to have infinite slope (though zero value) at the blade tip. Several schemes can deal with this problem; in a lifting line approach the

best seems to be assuming a reasonable functional form for $\Gamma(\rho)$ which has large negative, but finite, slope at $\rho = \rho_a$. Reissner proposed that $\Gamma = g\rho^p(\rho_a^q - \rho^q)$, which makes Γ zero at the hub and tip as required, but, unless $p+q=1$, the slope remains finite everywhere on the blade.

The Compressible Potential

A general solution to the steady, compressible, potential equation for the flow about a propeller may be obtained through separation of variables. The resulting series solution has the form:

$$\varphi = \sum_{n=0}^{\infty} A_n R_n(\rho) Z_n(z) e^{inB\theta}; \qquad (3.3)$$

with

$$R_n(\rho) = C_{nB}(\rho\sqrt{M^2n^2B^2 + \lambda_n^2},$$

and

$$Z_n(z) = exp\{i\frac{nB}{\rho s^2} \pm \frac{1}{\beta}\sqrt{\lambda_n^2 - \frac{n^2B^2M^2}{\rho_s^2}}\}z.$$

C_{nB} represents a linear combination of solutions to Bessel's equation, λ_n is the separation constant, or eigenvalue, and $\rho_s \equiv \beta/M$ is the dimensionless radius at which the local freestream velocity becomes sonic. Applying the boundary condition requiring finiteness of φ at $\rho = 0$ gives

$$R_n(\rho) = J_{nB}(\rho\sqrt{M^2n^2B^2 + \lambda_n^2}). \qquad (3.4)$$

A separated solution in a slightly different form from that given above was first proposed by Busemann[23].

Because of the behavior of the J-Bessel function as its argument approaches infinity, substitution of (3.4) into (3.3) above will cause automatic satisfaction of the radiation boundary condition. This leaves no mechanism for determining values for the eigenvalues, λ_n; in fact, the notion of the eigenvalue has no real meaning for problems of infinite domain. Therefore, the solution must be obtained using a method other than a simple separation of variables.

Due to periodicity in the angular coordinate, the expected solution to the partial differential equation has the form:

$$\varphi = \sum_{n=0}^{\infty} \varphi_n(\rho, z) e^{inB\theta}$$

Substituting this into the PDE gives

$$\varphi_{n\rho\rho} + \frac{1}{\rho}\varphi_{n\rho} - n^2B^2\frac{1}{\rho^2}(1+\rho^2M^2)\varphi_n = -\beta^2\varphi_{nzz} + 2inBM^2\varphi_{nz}.$$

Performing a Hankel transform on this equation gives

$$\beta^2\bar{\varphi}_{zz} - 2inBM^2\bar{\varphi}_z - (\gamma^2 - n^2B^2M^2)\bar{\varphi} = 0,$$

a second order, ordinary differential equation for the Hankel-transformed potential, $\bar{\varphi}$. The Hankel parameter, γ, appears only parametrically. The solution to this equation is easily obtained:

$$\bar{\varphi}_n(z;\gamma) = A_n exp\left\{\left[i\frac{nB}{\rho_s^2} \pm \frac{1}{\beta}\sqrt{\gamma^2 - \frac{n^2B^2}{\rho_s^2}}\right]z\right\}.$$

Inverting this transformed solution results in

$$\varphi_n(\rho, z) = \int_o^{\infty} A_n(\gamma)\gamma J_{nB}(\gamma\rho) * exp\left\{\left[i\frac{nB}{\rho_s^2} \pm \frac{1}{\beta}\sqrt{\gamma^2 - \frac{n^2B^2}{\rho_s^2}}\right]z\right\}d\gamma.$$

The complete solution to the compressible potential equation is, then

$$\varphi(\rho, z, \theta) = \sum_{n=o}^{\infty} e^{inB\theta}\int_o^{\infty} A_n(\gamma)\gamma J_{nB}(\gamma\rho) * exp\left\{\left[i\frac{nB}{\rho_s^2} \pm \frac{1}{\beta}\sqrt{\gamma^2 - \frac{n^2B^2}{\rho_s^2}}\right]z\right\}d\gamma.$$

It remains to determine the unknown "constants," $A_n(\gamma)$.

Applying Boundary Conditions

In order to satisfy the continuity conditons described by equations (3.2.a,b) the incompressible potential must be reformulated so that it is compatible with the compressible potential. Recall the current form of the incompressible solution:

$$\varphi_i = -\frac{B}{2\pi}\Gamma(\rho)(\theta - z) - \sum_{n=1}^{\infty} R_n(\rho) sin\ nB(\theta - z).$$

Using Hankel's integral (Watson,[30] eq. (14.3.3)), $\Gamma(\rho)$ can be rewritten as

$$\Gamma(\rho) = \int_o^{\infty} \gamma \int_o^{\infty} \Gamma(s) s J_{nB}(\gamma s) ds J_{nB}(\gamma\rho) d\gamma.$$

Then, expanding $(\theta - z)$ in a Fourier sine series, the first term in φ_i becomes:

$$\varphi_{io} = \frac{B}{2\pi}\sum_{n=1}^{\infty}\frac{2(-1)^n}{nB} sin\ nB(\theta - z) * \int_o^{\infty} \gamma\Gamma_n'(\gamma) J_{nB}(\gamma\rho) d\gamma,$$

where

$$\Gamma_n' \equiv \int_o^{\infty} \Gamma(s) s J_{nB}(\gamma s) ds.$$

The remaining continuous terms in the incompressible potential can also be rewritten using Hankel's Integral.

This, along with reconstruing the sine as an exponential, gives

$$\begin{aligned}\varphi_i &= \varphi_{io} + \varphi_{i1} \\ &= -\frac{iB}{2\pi}\sum_{n=1}^{\infty}\frac{2(-1)^n}{nB}e^{inB(\theta-z)}\int_o^\infty \gamma\Gamma_n'(\gamma)J_{nB}(\gamma\rho)d\gamma \\ &\quad + i\sum_{n=1}^{\infty}e^{inB(\theta-z)}\int_o^\infty \gamma R_n'(\gamma)J_{nB}(\gamma\rho)d\gamma,\end{aligned}$$

where

$$R_n' \equiv \int_o^\infty R_n(s)sJ_{nB}(\gamma s)ds.$$

The simplest matching procedure is modelled after that which Davidson employed for solution in a wind tunnel. Let the "constant" term in the compressible solution have the form $A_o(\gamma) + A_n(\gamma) + B_n(\gamma)$ where now, $n = 1, 2, 3, \ldots$ Generally, the first incompressible series will be matched with the A_n compressible series, and the second incompressible series with the B_n compressible series. This leaves the zero term in the compressible series which can be incorporated into the former matching by making

$$\left.\begin{aligned}\varphi_{i_o} + \varphi_{c_A}^- &= \varphi_{c_A}^+ \\ \varphi_{c_o}^- &= \varphi_{c_o}^+ \\ \frac{\partial}{\partial z}(\varphi_{i_o} + \varphi_{c_o}^-) &= \frac{\partial}{\partial z}\varphi_{c_o}^+ \\ \frac{\partial}{\partial z}\varphi_{c_A} &= \frac{\partial}{\partial z}\varphi_{c_A}^+\end{aligned}\right\} \text{at } z = 0.$$

(See symbol list for terminology clarification.) Application of the matching conditions at $z = 0$ determines the coefficients found in table 3.1.

Convergence of the Integrals.

Table 3.1 completes the solution for the compressible velocity potential except for the value of the unknown circulation distribution, $\Gamma(\rho)$. However, it is possible to determine the convergence of the integrals without complete knowledge of the circulation function.

In general, the complete compressible potential looks like

$$\begin{aligned}\varphi_c^{\pm} &= \int_o^\infty A_o(\gamma)\gamma J_o(\gamma\rho)e^{\pm(\gamma/\rho z)}d\gamma \\ &\quad + \sum_{n=1}^{\infty}e^{inB\theta}\int_o^\infty (A_n(\gamma) + B_n(\gamma))\gamma J_{nB}(\gamma\rho)* \\ &\quad exp\left\{\left[\frac{inB}{\rho_s^2} \pm \frac{1}{\beta}\sqrt{\gamma^2 - \frac{n^2B^2}{\rho_s^2}}\right]z\right\}d\gamma.\end{aligned} \tag{3.5}$$

From Gradshteyn and Ryzhik,[31] 6.561.14, the integral,

$$\int_o^\infty \chi^\mu J_\nu(a\chi)d\chi,$$

converges for $\mu < \frac{1}{2}$. Thus, as long as the function multiplying $J_{nB}(\gamma_\rho)$ in each of the above integrals behaves such that it is less than $\sqrt{\chi}$, the integral converges.

Determining the behavior of the multiplying function requires knowledge of how $\Gamma_n'(\gamma)$ and $R_n'(\gamma)$ behave. Recall that

$$\Gamma_n'(\gamma) = \int_o^\infty \Gamma_n(s)sJ_{nB}(\gamma s)ds.$$

However, $\Gamma_n(s) = 0$ for $s > \rho_a$, so the upper integration limit becomes ρ_a. Then, invoking the mean value theorem,

$$\Gamma_n'(\gamma) = \rho_a\Gamma_n(s_1)s_1J_{nB}(\gamma s_1) \tag{3.6.1}$$

for some s_1 such that $0 \le s_1 \le \rho_a$. In a similar, but somewhat more involved manner,

$$R_n'(\gamma) = C_1\frac{\gamma^{nB}}{(nB)^{nB}(\gamma^2 + n^2B^2)} + C_2s_2J_{nB}(s_2\gamma) \tag{3.6.2}$$

where C_1 and C_2 are constants, and $0 \le s_2 \le \rho_a$.

It is evident by observation that the integrals converge for all $z \neq 0$ as the receding exponential dies out more quickly than any power of γ contributed by the A_o, A_n, or B_n grows. The first integral (zero term in the series) converges even for $z = 0$ since the γ in the denominator of A_o cancels that in the integrand, and $J_{nB}(s\gamma)$ behaves asymptotically like $\sqrt{2/\pi s\gamma}$ for large γ. (See Abramowitz and Stegun[32], 9.3.1.)

Four integrals remain – those corresponding to both real and imaginary parts of both $A_n(\gamma)$ and $B_n(\gamma)$ as z goes to zero. The imaginary parts stand to cause the greatest problem as they do not contain the order–lowering $\sqrt{\gamma^2 - n^2B^2/\rho_s^2}$ in their denominators. Writing the imaginary integrands as γ gets large, the integrals of interest become:

$$\int_o^\infty \gamma J_{nB}(\gamma s_1)J_{nB}(\gamma\rho)e^{-\gamma z}d\gamma = I_1,$$

and

$$\int_o^\infty \gamma^{nB-1}J_{nB}(\gamma\rho)e^{-\gamma z}d\gamma = I_2.$$

From Gradshteyn and Ryzhik, 6.633.2 and 6.621.4,

$$I_1 = \frac{1}{2z}exp(-\frac{\rho^2 + s_1^2}{4z})I_{nB}(\frac{\rho s_1}{2z}),$$

and

$$I_2 = (-1)^{nB-1}\rho^{-nB}\frac{d^{nB-1}}{dz^{nB-1}}\left\{\frac{(\sqrt{z^2+\rho^2} - z)^{nB}}{\sqrt{z^2+\rho^2}}\right\}.$$

Now, taking the limits as $z \to 0$, I_1 goes to zero and I_2 takes on a finite value depending on the order of the Bessel function For example, for $n = 1$ and $B = 2$, $\lim_{z\to 0} I_2 = 2/\rho^2$. The integrals involving the real parts of $A_n(\gamma)$ and $B_n(\gamma)$ can be shown to converge using a similar approach.

4. Results and Discussion

The previous development derives and solves for an expression for the total perturbation velocity potential in

	Forward ($z \leq 0$)	Behind ($z \geq 0$)
A_0	$\frac{B}{2\pi}\ \frac{\beta}{2\gamma}\ \Gamma_0'(\gamma)$	$\frac{B}{2\pi}\ \frac{\beta}{2\gamma}\ \Gamma_0'(\gamma)$
A_n	$\frac{B}{2\pi}\ \frac{2(-1)^n}{nB}\ \frac{\Gamma_n'(\gamma)}{2}\left[-i - \frac{nB\beta}{\rho_s^2\sqrt{\gamma^2-\frac{n^2B^2}{\rho_s^2}}}\right]$	$\frac{B}{2\pi}\ \frac{2(-1)^n}{nB}\ \frac{\Gamma_n'(\gamma)}{2}\left[i - \frac{nB\beta}{\rho_s^2\sqrt{\gamma^2-\frac{n^2B^2}{\rho_s^2}}}\right]$
B_n	$-\frac{R_n'(\gamma)}{2}\left[-i - \frac{nB}{\beta\sqrt{\gamma^2-\frac{n^2B^2}{\rho_s^2}}}\right]$	$-\frac{R_n'(\gamma)}{2}\left[i - \frac{nB}{\beta\sqrt{\gamma^2-\frac{n^2B^2}{\rho_s^2}}}\right]$

Table 3.1 - Coefficients for Compressible Velocity Potential Series

terms of the unknown circulation distribution, $\Gamma(\rho)$. In general, applying the boundary condition requiring no fluid velocity normal to the propeller blade determines this final unknown. This condition may be expressed as

$$u_z \cos\epsilon - u_\theta \sin\epsilon = W\alpha \quad for \quad z,\theta \rightarrow blade, \qquad (4.1)$$

for the simple case of uncambered, thin airfoil sections. u_z and u_θ are the perturbation velocities, achieved by differentiating the velocity potential. $u_z, u_\theta, \epsilon, W$, and α are all functions of radial position.

In the lifting line approximation, there is no blade at which to apply condition (4.1). Instead, the condition given by Reissner[3] must be used. Referring to figure 4.1, this condition is given as

$$\alpha = \alpha_g - \frac{v_i}{W} \quad at \quad z \rightarrow 0, \theta \rightarrow \frac{\pi}{B}. \qquad (4.2)$$

α_g is the geometric angle of attack, and v_i is the induced velocity perpendicular to W.

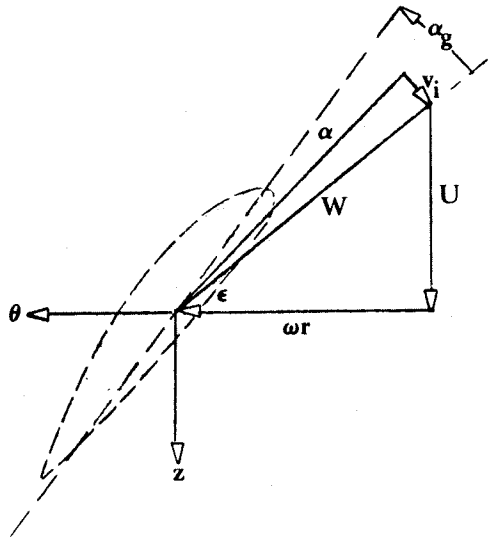

Figure 4.1 -- Velocities at the Blade

Two well known relations assist in reducing (4.2) to usable form: $\ell = \mu W\Gamma$ and $\ell = \frac{\mu}{2}W^2 c\, c_{\ell_\alpha}\alpha$, where $\ell \equiv$ lift per unit radius, $\mu \equiv$ density, $c_{\ell_\alpha} \equiv$ section lift curve slope, and $c \equiv$ blade chord. Combining these two expressions gives $\alpha = 2\Gamma/Wcc_{\ell_\alpha}$. Substituting this into (4.2) gives

$$\frac{v_i}{W} + \frac{2\Gamma}{\rho_a \bar{c} c_{\ell_\alpha}}\frac{U}{W} = \alpha_g, \ z \rightarrow 0, \ \theta \rightarrow \frac{\pi}{B}, \qquad (4.3)$$

where $\bar{c} \equiv c/R$, an inverse "blade aspect ratio." Note that $v_i = u_z \cos\epsilon - u_\theta \sin\epsilon$, as before.

Condition (4.3) introduces two parameters, $\bar{c}$ and c_{ℓ_α}. $\bar{c}$ is easily estimated for a typical propeller blade; however, c_{ℓ_α} is not known in advance for compressible flow. It is assumed here that an estimate of c_{ℓ_α} based on strip theory will introduce only minimal error.

By defining $\varphi^* = \frac{\omega}{U^2}\varphi$ and $\Gamma^* = \frac{\omega}{U^2}\Gamma$, (4.3) can be written in dimensionless form:

$$\rho\frac{\partial\varphi^*}{\partial z} - \frac{1}{\rho}\frac{\partial\varphi^*}{\partial\theta} + \frac{2\Gamma^*}{\rho\bar{c}\, c_{\ell_\alpha}} = (1+\rho^2)\alpha_g, \quad z \rightarrow 0, \theta \rightarrow \frac{\pi}{B}. \qquad (4.4)$$

Carrying out the derivatives results in the following expressions for the perturbation velocities:

$$u_z^* = \left.\frac{\partial \varphi^*}{\partial z}\right|_{\substack{z\to 0\\ \theta \to \frac{x}{B}}} = \frac{B\Gamma^*}{4\pi} + \sum_{n=1}^{\infty}(-1)^n nB\frac{R_n^*}{2} + \sum_{n=1}^{\infty}\frac{1}{2\pi n\beta}\int_o^{\gamma_{ns}}\Gamma_n^{*\prime}\left[\frac{\gamma^2-\beta^2\gamma_{ns}^2}{\sqrt{\gamma_{ns}^2-\gamma^2}}\right]\gamma J_{nB}(\gamma\rho)d\gamma + \sum_{n=1}^{\infty}\frac{(-1)^n}{2\beta}\int_o^{\gamma_{ns}} R_n^{*\prime}\frac{\gamma^3}{\sqrt{\gamma_{ns}^2-\gamma^2}}J_{nB}(\gamma\rho)d\gamma; \tag{4.5.a}$$

$$\rho u_\theta^* = \left.\frac{\partial \varphi^*}{\partial \theta}\right|_{\substack{z\to 0\\ \theta \to \frac{x}{B}}} = -\frac{B\Gamma^*}{4\pi} - \sum_{n=1}^{\infty}(-1)^n nB\frac{R_n^*}{2} - \sum_{n=1}^{\infty}(-1)^n\frac{B\beta}{2\pi\rho_s^2}\int_o^{\gamma_{ns}}\Gamma_n^{*\prime}\frac{\gamma}{\sqrt{\gamma_{ns}^2-\gamma^2}}J_{nB}(\gamma\rho)d\gamma - \sum_{n=1}^{\infty}(-1)^n\frac{n^2B^2}{2\beta}\int_o^{\gamma_{ns}} R_n^{*\prime}\frac{\gamma}{\sqrt{\gamma_{ns}^2-\gamma^2}}J_{nB}(\gamma\rho)d\gamma. \tag{4.5.b}$$

In the above, $\gamma_{ns} = nB/\rho s$ and $R_n^{*\prime} = R_n'(\Gamma^*)$.

Since the velocities are evaluated at the lifting line (that is, at a vortex line representing the propeller blade), some terms in equations (4.5.a,b) must include the self induction by the lifting line. Those terms, characterized by the Γ_n' terms under the integral sign, must be discarded in order to obtain the proper induced velocities at the lifting line. Davidson[22] provides further explanation of this point. The discarding of terms could be avoided if the control points were chosen using a Weissinger–type approach, but substantial complexity is added to the expressions for the induced velocities using that procedure.

Equations (4.4) and (4.5.a,b) represent, in effect, an integral equation in the unknown, $\Gamma^*(\rho)$. A useful method for solving this type of equation involves determining a series "shape function" for Γ^* with unknown coefficients. The left–hand–side of (4.4) is determined using each of K shape functions at K control points on the blade. This procedure results in a $K \times K$ system of equations for the K unknown coefficients of the shape function.

The shape functions used here are modeled after those suggested by Reissner. Using $\Gamma = \sum_{k=1}^{k} g_K \rho^{(k+2)}(\rho_o - \rho)$, results in the linear equation

$$[\Re]\vec{g} = \vec{\alpha}$$

where $[\Re]$ is a $K \times K$ matrix formed by substituting K shape functions into the left hand side of (4.4) for K control points. $\vec{g}$ is the unknown vector of coefficients, g_k, and $\vec{\alpha}$ is the vector formed by specifying the geometric twist at K control points.

Figure 4.2 illustrates some typical results for this method. The figure shows Γ^* distributions for 4, 6, and 10 equally spaced control points. The solution appears to be converging as K increases. It is logical that a propeller may require more control points than a wing for convergence due to the variation in the freestream along the radius. Convergence may be enhanced by concentrating control points near the blade tip.

Figure 4.2 -

COMPRESSIBLE CIRCULATION DISTRIBUTION
M = 0.65
ρ_s = 1

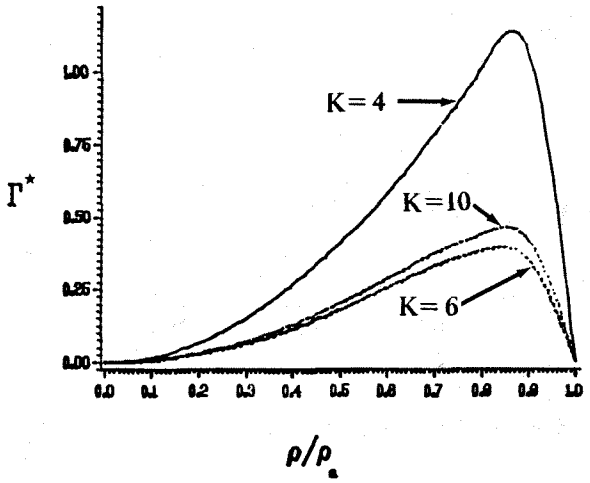

Inspection of (4.5.a,b) reveals that the induced velocities have the form $u = u_i + \Delta u_c$ where u_i is the induced velocity for incompressible flow (see Reissner[3]), and Δu_c represents a change in induced velocity due to compressibility. However, this "compressibility correction" holds only for propellers with common circulation distributions – a quantity much more difficult to specify than twist distribution – and, thus, is not particularly useful as a correction to incompressible results. Figure 4.3 compares the compressible and incompressible circulation distributions for propellers with the same geometric angle of attack distribution. As expected, the compressible case has a greater magnitude of circulation, paralleling the same trend due to Mach number which occurs for straight wings.

Figure 4.3 -

CIRCULATION DISTRIBUTIONS
COMPRESSIBLE AND INCOMPRESSIBLE
ρ_s = 1
K = 10

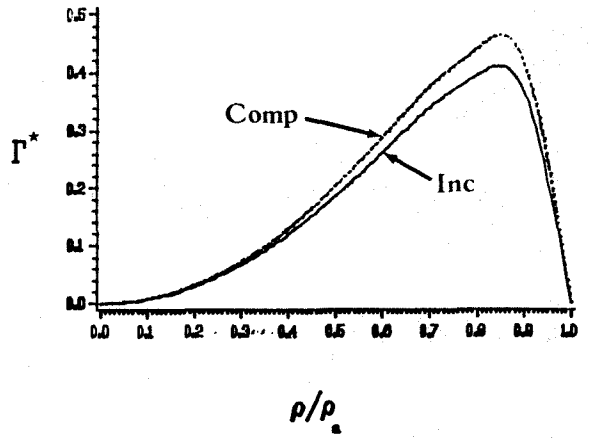

Though it is difficult to predict analytically the convergence of the important compressible parts of (4.5.a, b), the numerical computations indicate good convergence within five terms. Table 4.1 shows the relative values of the first eight terms in the series for both u_{θ_c} and u_{z_c} for a typical circulation distribution at $\rho = .5\rho_a$.

n	$\left(\frac{A_n}{A_1}\right)_z$	$\left(\frac{A_n}{A_1}\right)_\theta$
1	1.0000	1.0000
2	.8092	.7573
3	$.8493 \times 10^{-1}$	$.7733 \times 10^{-1}$
4	$.9258 \times 10^{-3}$	$.8493 \times 10^{-3}$
5	$.1213 \times 10^{-3}$	$.1096 \times 10^{-3}$
6	$.1762 \times 10^{-4}$	$.1573 \times 10^{-4}$
7	$.2323 \times 10^{-5}$	$.2069 \times 10^{-5}$
8	$.3388 \times 10^{-6}$	$.3042 \times 10^{-6}$

Table 4.1 - Convergence of $z-$ and $\theta-$velocity series.

Conclusion

The results obtained above inspire confidence in the derivation and the solution methods since a) they show convergence in both the series solutions for the velocities and the shape function solutions, and b) they show trends anticipated from wing theory. Of course, a favorable comparison with experiment would reinforce confidence in the method.

Further results are easily obtained and are shortly forthcoming. These include:

a) thrust and torque distributions,

b) efficiency calculations, and

c) effects of changing Mach number and advance ratio.

The Weissinger boundary condition should also be studied for accuracy improvement. In addition, a viscous drag correction term must be included to correctly predict the thrust and torque distributions, particularly for a compressible propeller analysis.

References

1. Jones, R. T., Classical Aerodynamic Theory, NASA Reference Publication 1050, 1979.
2. Goldstein, S., "On the Vortex Theory of Screw Propellers," Proc . Roy. Sec. (London), Ser. A, Vol. 123, No. 792, Apr. 1929, pp. 440–465.
3. Reissner, H., "On the Relation Between Thrust and Torque Distribution and the Dimensions and Arrangement of Propeller Blades, Phil. Mag., Ser. 7, Vol. 24, No. 163, Nov. 1937, pp. 745–771.
4. Theodorsen, Theodore, Theory of Propellers, Mc Graw-Hill, New York, 1948.
5. Glauert, H., "Airplane Propellers," Div. L, Aerodynamic Theory, W. F. Durand, ed., Vol. IV, pp. 324–341, Julius Springer, Berlin, 1935.
6. Shiao, Ta–Ching, "Aerodynamic Analysis of Propeller – Type Windmills with Helical Trailing Vortices," Ph. D. Thesis, University of Colorado, Boulder, 1980.
7. Chang, Li Ko, "The Theoretical Performance of High Efficiency Propellers," Ph. D. Thesis, Purdue University, 1980.
8. Sullivan, J. P., Chang, L. K., and Miller, C. J., "The Effect of Proplets and Bi–Blades on the Performance and Noise of Propellers," SAE Paper 810600, 1981.
9. Glatt, L., Kosmatka, J., Swigart, R., Wong, E., Crawford, D., and Neuman, H., "The Development of a Generalized Advanced Propeller Analysi System," AIAA–83–2466, 1983.
10. Pierce, G. Alvin, and Vaidyanatham, Anand R., "Helicopter Rotor Loads Using a Matched Asymptotic Expansion Technique," NASA CR 165742, 1981.
11. Johansson, Bo C. A., "Lifting Line Theory for a Rotor in Vertical Climb," Aero. Res. Inst., Sweden (FFA), Rept. 118, 1971.
12. Bober, Lawrence J., Chaussee, Denny S., and Kutler, Paul, "Prediction of High Speed Propeller Flow Fields Using a Three–Dimensional Euler Analysis," NASA TM 83065, 1983.
13. Ffowcs Williams, J. E., and Hawkings, D. L., "Sound Generation by Turbulence and Surfaces in Arbitrary Motion," Phil. Trans. Roy. Soc. (London), Ser. A, Vol. 264, May 8, 1969, pp. 321–342.
14. Farassat, F., "Theory of Noise Generation From Moving Bodies With an Application to Helicopter Rotors," NASA TR R–451, 1975.
15. Schmitz, Fredric H., and Yu, Yung H., "Compressible Aerodynamics and Noise of Rotary Wing Aircraft," Course Notes, Department of Aeronautics and Astronautics, Stanford University, 1982.
16. Dat, Rolland, "La Théorie de la Surface Portante Appliquée a l'Aile Fixe et a l'Hélice," La Récherche Aérospatiale, Année 1973, No. 4 (Juillet–Aout), pp. 245 á 254.
17. Runyan, Harry L., "Unsteady Lifting Surface Theory Applied t a Propeller and Helicopter Rotor," Ph. D. Thesis, Loughborough University of Technology (Loughborough, England), 1973.
18. Kerwin, J. E., "The Solution of Propeller Lifting Surface Problems by Vortex Lattice Methods," Dept. of Naval Architecture, MIT, 1961.
19. Summa, J. M., "Potential Flow About Three-Dimensional Streamlined Lifting Configurations with Application to Wings and Rotors," Ph. D. Thesis, Stanford University, 1974.
20. Jacobs, W. R., and Tsakonas, S., "Propeller–Induced Velocit Field by Means of Unsteady Lifting Surface Theory," Stevens Institute of Technology, Davidson Laboratory Report SIT–DL–72–1588, 1972.
21. Long, Lyle N., "The Compressible Aerodynamics of Rotating Blades Based on an Acoustic Formulation," NASA TP 2197, 1983.

22. Davidson, R. E., "Linearized Potential Theory of Propeller Induction in a Compressible Flow," NACA TN 2983, 1953.

23. Busemann, Adolf, "Theory of the Propeller in Compressible Flow," presented at Third Midwestern Conference on Fluid Mechanics (Minneapolis, Minn.), Mar. 22–24, 1953.

24. Dowell, E. H., Curtiss, H. C., Scanlan, R. H., and Sisto, Fernando, A Modern Course in Aeroelasticity, Sijthoff and Noordhoff, Alphen aan den Rijn, The Netherlands, 1980.

25. von Mises, Richards, Mathematical Theory of Compressible Fluid Flow. New York: Academic Press, 1958.

26. Hayes, Wallace D. and Probstein, Ronald F., Hypersonic Flow Theory, Volume I, Inviscid Flows. New York: Academic Press, 1966.

27. Courant, R. and Friedrichs, K. O., Supersonic Flow and Shock Waves. New York: Interscience Publishers, Inc., 1948.

28. Sauerwein, Harry Jr., The Calculation of Two– and Three–Dimensional Inviscid Unsteady Flows by the Method of Characteristics. Ph. D. Thesis, Massachusetts Institute of Technology, 1964.

29. Courant, R. and Hilbert, D., Methods of Mathematical Physics, Volume II, Interscience Publishers, 1962.

30. Watson, G. N., A Treatise on the Theory of Bessel Functions, Second Edition, Cambridge University Press, 1952.

31. Gradshteyn, I. S. and Ryzhik, I. M., Table of Integrals, Series, and Products, Fourth Edition, Academic Press, 1965.

32. Abramowitz, Milton and Stegun, Irene A., Handbook of Mathematical Functions with Formulas, Graphs and Mathematical Tables, National Bureau of Standards, Washington, D. C. 1972.